Advances in Biological Chemistry, 2012, 2, 123-131 **ABC**
http://dx.doi.org/10.4236/abc.2012.22015 Published Online May 2012 (http://www.SciRP.org/journal/abc/)

Two disulfide mutants in domain I of *Bacillus thuringiensis* Cry3Aa δ-endotoxin increase stability with no effect on toxicity*

Sheng-Jiun Wu[1], Alvaro M. Florez[2], Bradley J. Homoelle[1], Donald H. Dean[1#], Oscar Alzate[3,4,5,#]

[1]Biochemistry Department, Ohio State University, Columbus, USA
[2]Laboratorio de Biología Molecular y Biotecnología, Facultad de Medicina, Universidad de Santander (UDES), Bucaramanga, Colombia
[3]Department of Cell and Developmental Biology, University of North Carolina, Chapel Hill, USA
[4]Universidad Pontificia Bolivariana, Medellín, Colombia
[5]Biophysics Program, Ohio State University, Columbus, USA
Email: [#]alzate@med.unc.edu, [#]dean.10@osu.edu

Received 28 January 2012; revised 1 March 2012; accepted 10 March 2012

ABSTRACT

To increase protein stability and test protein function, three double-cysteine mutations were individually introduced by protein engineering into the cysteine-free Cry3Aa δ-endotoxin from *Bacillus thuringiensis*. These mutations were designed to create disulfide bonds between α-helices 2 and 5 (positions 110 - 193), and α-helices 5 and 7 (positions 195 - 276 and 198 - 276). Comparison of the CD spectra of the wild-type and the double-cysteine mutant proteins indicates a tighter helical packing consistent with formation of at least two of the disulfide bonds between the central and the outer helices. Thermal stability analysis indicates that potential covalent linkages between the central α-helix 5 and the other helices increase resistance to thermal denaturation by 10˚C to 14˚C compared to the thermal stability of the wild-type protein. Spectroscopic analysis of the disulfide-specific absorbance band indicates that the double mutant proteins are more stable to temperature and denaturant (guanidine hydrochloride) than the wild-type protein, as a result of the formation of two of the disulfide bridges. These results indicate that the double mutations $M_{110}C/F_{193}C$ and $A_{198}C/V_{276}C$ successfully established disulfide bonds, resulting in a more stable structure of the entire toxin. Despite the increase in stability and structural changes introduced by the disulfide bonds, no effect on toxicity was observed. A possible mechanism involving the insertion of all of domain I of Cry3Aa toxin into the target membrane accounts for these observations.

Keywords: Disulfide Bonds; CD Spectra; Cry3Aa; Site Directed Mutagenesis

1. INTRODUCTION

Protein engineering is a powerful tool for modifying the properties of polypeptide molecules. One particular application of protein engineering is sequence alteration to enhance protein stability in order to broaden their utility in commercial and medical applications. It is known that the tertiary structure of native proteins is defined by a number of weak interactions including: hydrophobic interactions [1], salt bridges [2], weakly polar interactions [3], and hydrogen bonding [4]. Additionally, disulfide bonds can make a substantial contribution to the overall protein resistance to adverse environmental factors [5], and can play an important role in specific aspects of structural stability [6].

There have been reports in which protein stability of Cry1Aa protein has been improved by introducing artificial disulfide bridges [7,8]. Introduction of new disulfide bridges in proteins does not always result in increased stability to thermal or chemical inactivation, however. It has been suggested that one reason for this is that disulfide bridges in native proteins have special geometries which may be difficult to achieve in engineered proteins [9].

Several mechanisms have been proposed for the insertion of δ-endotoxins into the insect plasma membrane. The "penknife" [10] and "umbrella" models [11] are supported by changes in the distribution of the hydrophobic faces of the helices in domain I. Both models involve separation of the α-helices from the α-helical bundle, followed by their insertion into the target membranes resulting in the formation of ion pores. Other

*Engineered disulfide bridges in Cry3Aa.
#Corresponding authors.

studies have proposed that the whole domain I inserts into the protein, without α-helical separation [7,12-17]. There is also evidence that other domains of the protein are able to insert into membrane [16], and that several mutations in the domain I (α-helices 3 and 4) affect oligomer formation [18-20]. Several disulfide-bridge mutations generated by protein engineering which are related to the membrane partitioning mechanisms of Cry toxins are reviewed in [21]. An intermediate step has been proposed in which the oligomerization occurs in tetramers after the hairpins from α-helices 3 and 4 are inserted into the membrane [22,23]. At the present time no single model can account for all the experimental observations.

Based on the crystal structure of Cry3Aa, we designed and separately introduced three double cysteine mutations expected to create disulfide bonds into the Cry3Aa protein. This was possible without prior manipulation of the protein because the Cry3Aa wild type protein does not contain disulfide bridges [11]. Structural analysis and site directed mutagenesis were used to engineer disulfide bonds between α-helices 2 and 5, and between α-helices5 and 7 of Cry3Aa. It was expected that these bonds would modify the function of Cry3Aa and that that modification would be reflected in altered toxicity. In this study, we analyzed the effects of these disulfide mutants on protein stability. The data indicate that the thermal stability of Cry3Aa can be increased significantly by introduction of the disulfide bonds in domain I, without significant changes to protein toxicity.

2. MATERIALS AND METHODS

2.1. Design of Disulfide Bridges

Candidate residues for the introduction of disulfide bridges were examined as previously described [7,8]. First, the coordinates for Cry3Aa were retrieved from the Protein Data Bank (http://www.rcsb.org/pdb/home/homedo PDB code: 1DLC; [11]). The structure of Cry3Aa was analyzed with the computer program HyperChem (Hypercube, Inc. Gainesville, FL) on a Silicon Graphics Iris workstation (Silicon Graphics, Fremont, CA). The desired positions for the engineered disulfide bonds were between the central α-helix 5 and the outer α-helices of domain I (**Figure 1**). The following criteria were used to constrain the selection of candidate amino acids for mutagenesis: 1) the distance between the α-carbon of the residue on α-helix 5 and that on the outer α-helix must be less than 6 Å; and 2) the α-carbon atoms on both residues had to be oriented toward each other. Next, after *in silico* mutagenesis, the resulting structures were geometry- and energy-minimized. Geometry optimization for all the residues within a sphere of a 7 Å radius from the α-carbon of the selected amino acid residues on α-helix 5 was carried out using the AMBER algorithm [24]. The global

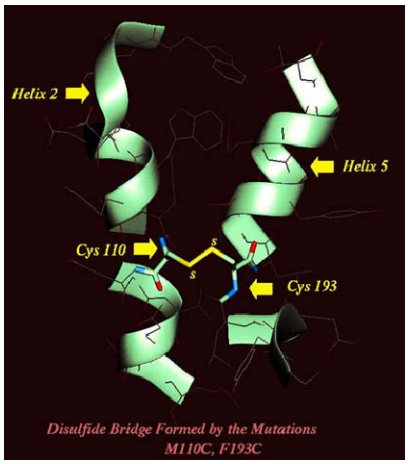

(a)

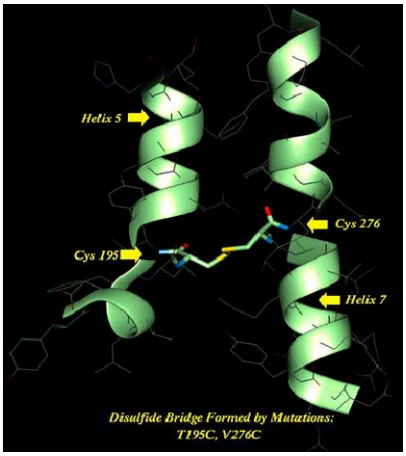

(b)

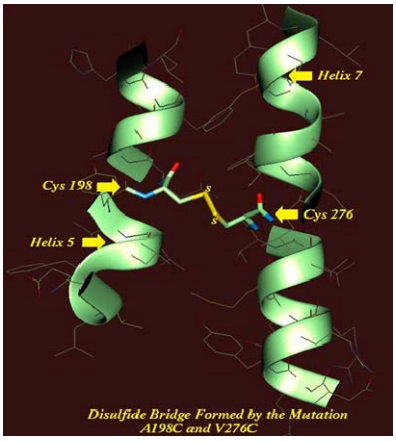

(c)

Figure 1. Molecular representation of potential disulfide bonds in the domain I of the Cry3Aa δ-endotoxin. (a) Schematic ribbon representation of DS1 disulfide bond, $M_{110}C/F_{193}C$, between α-helices 2 and 5; (b) DS2 disulfide bridge, $T_{195}C/V_{276}C$, between α-helices 5 and 7; (c) Representation of the DS3 disulfide bond, $A_{198}C/V_{276}C$, between α-helices 5 and 7.

energy of the mutant protein after the optimization of disulfide mutants was compared to the global energy calculated for the wild-type toxin. Finally, root mean square tests were carried out on the mutant forms to determine the optimum conformations resulting from replacing cysteine residues on the wild-type Cry3Aa structure. Candidate amino acid residues for mutagenesis were simulated with Quanta 4.0 (Molecular Simulations Inc., Waltham, MA) and tested to determine that criteria 1 and 2 were met.

2.2. Construction of Mutant Proteins and Toxicity Assays

The construction of pOS4601 which carries the Cry3Aa gene and its expression in *Escherichia coli* was described in Wu and Dean [25]. The Cry3Aa gene was used as a template to introduce the mutations that should result in the formation of the three disulfide mutants by site-directed mutagenesis [26]: $M_{110}C$ and $F_{193}C$; $T_{195}C$ and $V_{276}C$; $A_{198}C$ and $V_{276}C$. The concentration of solubilized proteins was determined by Coomassie protein assay reagent (Thermo, Rockford, IL). The expression of wild-type and mutant toxins were determined by SDS-polyacrylamide gel (12.5%) electrophoresis (SDS-PAGE) [27]. The selected mutations for the construction of three mutant proteins, containing pairs of cysteines that could potentially form disulfide bonds and five single mutants as control proteins are summarized in **Table 1**. The force-feeding bioassay technique on beetle larvae of *T. molitor*, and the data analyses have been previously described [25].

2.3. Circular Dichroism (CD) Measurements

CD spectra were recorded on a Spex-CD6 spectropolarimeter (HORIBA Jobin-Yvon, Longjumeau, France) equipped with thermostatic control with a 1-cm path-length quartz cell (Hellma-Analytics, Müllheim, Germany), at room temperature (21˚C). CD data are presented as molar ellipticities, *i.e.*, deg·cm^2/dmol. The spectra were the average of 25 scans collected from 195 to 265 nm, recorded at 1 nm intervals at a scanning rate of 1 nm/min with a 2 msec time constant.

Thermal denaturation was determined by measuring the protein's secondary structure with CD. The spectra were recorded at a fixed wavelength of 222 nm (characteristic of the α-helix conformation) [28,29]. Temperature gradients from 40˚C to 82.5˚C were generated with a HP89090A Peltier temperature controller (Hewlett Packard, Santa Clara, CA) and a Lauda RC6 circulating water bath (Lauda-Königshofen, Germany). Heating and cooling rates were performed in steps of 2˚C, with a 20 min equilibration time. Data were recorded using the CD6 software supplied with the spectropolarimeter. The transition curves were normalized to the fraction of the folded protein using the standard equation: $F = ([\theta] - [\theta]_\upsilon)/([\theta]_v - [\theta]_\upsilon)$, where $[\theta]_n$ and $[\theta]_u$ represent the ellipticity values for fully-folded and fully-unfolded species, respectively; and $[\theta]$ is the observed ellipticity at 222 nm [28,29]. The concentration of the protein samples used for obtaining the CD spectra was 0.2 mg/mL in 10 mM

Table 1. Amino acid residues selected for construction of disulfide bridge mutants and toxicity assays to *Tenebrio molitor* larvae.

Protein	Selected amino acid residues	Location	Expression	LD*	(CL95)*	Relative toxicity
Wild-type Cry3Aa			++ (control)	11.4	(8.5 - 14.9)	1.0
Single mutants:						
Single mutant 1	$M_{110}C$	-Helix	++	11.7	(8.3 - 14.5)	1.0
Single mutant 2	$F_{193}C$	-Helix	-			
Single mutant 3	$T_{195}C$	-Helix	+	11.1	(7.8 - 13.4)	1.0
Single mutant 4	$A_{198}C$	-Helix	+	10.2	(7.1 - 14.5)	1.1
Single mutant 5	$V_{276}C$	-Helix	+	13.6	(10.3 - 17.7)	0.8
Disulfide mutants:						
DS1 mutant	$M_{110}C/F_{193}C$		+	12.7	(7.5 - 13.7)	0.9
DS2 mutant	$T_{195}C/V_{276}C$		+	10.3	(9.2 - 16.5)	1.1
DS3 mutant	$A_{198}C/V_{276}C$		+	9.6	(6.0 - 18.6)	1.2

*50% lethal doses (LD50) and 95% confidence limits (CL95) are expressed as µg per larva.

sodium carbonate buffer, pH 11.0.

2.4. UV Absorbance of Expected Disulfide Mutants

The UV absorbance was scanned from 200 to 314 nm and the peak intensity at 250 nm was recorded using a HP8452A Diode-Array spectrophotometer (Hewlett Packard, Santa Clara, CA). Temperature gradients from 25˚C to 100˚C were generated with a temperature-controlled circulating water bath (Lauda). Data were collected at 2.5˚C intervals. The concentration of the protein samples was 0.2 mg/mL in 10 mM sodium carbonate and 6 M guanidine hydrochloride (GnHCl) buffer, pH 11.0.

3. RESULTS

3.1. Expression of Mutant Proteins

Three double-cysteine mutants of the Cry3Aa protein were constructed which were expected to form disulfide bridges, referred to as DS1, DS2 and DS3 (**Table 1**). The expected disulfide bonds are indicated in the 3D structure of the toxin (**Figures 1 (a)-(c)**). There were also five proteins containing single amino acid mutations which were used as control proteins. These are $M_{110}C$, $F_{193}C$, $T_{195}C$, $A_{198}C$ and $V_{276}C$ (**Table 1**).

The expression of these mutant proteins was analyzed by SDS-PAGE (**Figure 2**). The predominant band of the expressed proteins displayed a 73-kDa apparent molecular weight. The average molecular weight of these proteins was reduced to approximately 67 kDa after treatment with the midgut juice of *T. molitor* larvae (**Figure 2**, **lane 6**). The single mutant, $F_{193}C$, did not express structurally-stable protein (**Figure 2**, **lane 3**), except when a counterpart mutation $M_{110}C$ was also introduced (**Figure 2**, **lane 7**). This may be evidence that the disulfide bridge was actually formed, and that it introduced an unexpected stability to the protein, rendering it resistant to proteolytic activity). All of the expected disulfide mutants produced structurally-stable proteins (**Figure 2**, **lanes 7-9**).

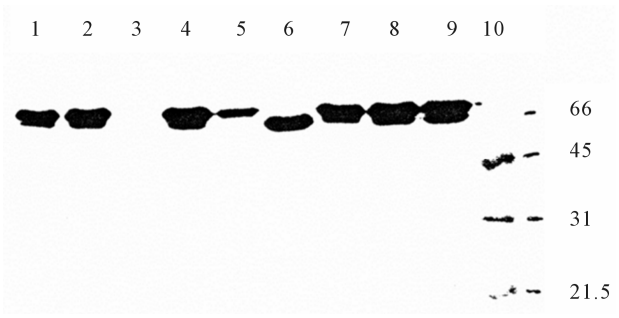

Figure 2. Coomassie blue stained 12.5% SDS-PAGE comparing the expression of wild-type Cry3Aa and disulfide mutant proteins. Lanes 1 to 5, single mutants: 1) $A_{198}C$; 2) $M_{110}C$; 3) $F_{193}C$; 4) $T_{195}C$; and 5) $V_{276}C$. Lane 6: wild-type Cry3Aa treated with *Tenebrio molitor* midgut juice. Lanes 7 to 9, double mutants: 7) DS1, $M_{110}C/F_{193}C$; 8) DS2, $T_{195}C/V_{276}C$; and 9) DS3, $A_{198}C/V_{276}C$. Lane 10: molecular weight protein markers (Bio-Rad, Hercules, CA). Positions of molecular weight markers are indicated in kDa to the right. Each lane contained 10 - 12 µg of protein.

3.2. Secondary Structure Analysis of Disulfide Mutants by CD Spectroscopy

The far-UV CD spectra for Cry3Aa and the double mutants showed a significant degree of α-helical structure (**Figure 3**). At 21˚C, the molar ellipticities of wild-type, DS1, DS2 and DS3 proteins at the minimum (*ca.* 220 nm), which is characteristic for an α-helix, are −23,367, −20,314, −21,619 and −21,619 deg·cm^2/dmol, respectively. Although these values for disulfide mutants decreased slightly, the changes are not statistically signifycant and the overall CD spectra of the wild-type and the mutant proteins were similar to one another. Further analysis of the spectrum between 200 and 240 nm (secondary structure analysis) showed that there were changes in molar ellipticity resulting from the introduction of double mutants, consistent with the formation of disulfide bridges in Cry3Aa. The parallel band reshifted from 211 for the wild-type protein to 213 for the DS2, and DS3 mutants and decreased in intensity from −22,322 to −20,516 deg·cm^2/dmol. However, the changes in sign of the π-π^* transition is at a lower wavelength (208 nm) for the DS1 mutant protein than for the wild-type.

The n-π^* transition (220 nm CD band) is a function of

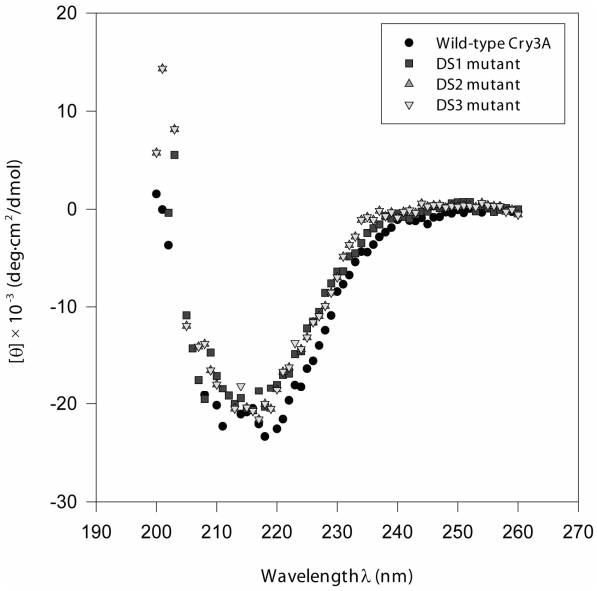

Figure 3. CD spectra of wild-type Cry3Aa and disulfide mutant proteins. Spectra were recorded at a protein concentration of 3 µM in 10 mM sodium carbonate buffer (pH 11.0), at 21˚C.

the α-helical content. The π-π^* excitation band at 208 nm polarizes parallel to the α-helical axis and is sensitive to whether the α-helix is monomeric or involved in tertiary contacts [30,31]. Thus, the ratio of $[\theta]_{220}/[\theta]_{208}$ is regarded as a measure of the degree of inter-helix coiling structure. The 220 to 208 nm ratio of ellipticities for Cry3Aa and the disulfide mutants were calculated and are summarized in **Table 2**. The ratio changes from 1.18 for wild-type protein to 1.34 for DS2 and DS3 mutants, while the ratio of ellipticity decreases to 0.92 for the DS1 mutant protein. These results suggest that α-helical structure in domain I of DS2 and DS3 proteins is slightly more closely-packed than in the wild-type protein.

3.3. Thermal Stability and Transition of Disulfide Mutants

To measure the structural stability and evaluate the nature of the folding/unfolding transition for disulfide mutants, the CD signal change at 222 nm was monitored. CD spectra for mutant proteins recorded at different temperatures show a significant increase in thermal stability, as evidenced by amplitude of the CD signal at 222 nm (**Figure 4**). The unfolding process is complete at 80˚C as the spectrum does not change when the temperature is increased to 85˚C. Assuming 100% and 0% folded structure at 40˚C and 80˚C, respectively, we calculated a melting temperature at the midpoint of the transition curve, $F = 0.5$ and $T = T_m$ (**Figure 4** and **Table 2**). The results showed that T_m increases by 10˚C to 14˚C as a result of the apparent introduction of the disulfide bonds. The thermal denaturation studies on the effect of the new inter-chain disulfide bonds in domain I suggest that the stability of Cry3Aa increases significantly, especially when the cysteine mutations are placed in the α-helices 5 and 7.

3.4. Guanidine Hydrochloride Induced Unfolding of Double Cysteine Mutants

To determine the contribution of the apparent disulfide bridges to the stability of the mutant proteins, the UV spectra in the presence of 6 M GnHCl were measured. It is well known that disulfide bonds display a weak absorbance band around 250 nm, where the disulfide group is the only significant chromophore [32]. In contrast to urea, GnHCl is a charged molecule and can potentially mask electrostatic interactions [33]. Therefore, the unfolding of wild-type and double cysteine mutants induced by GnHCl would result in a larger spectral change

Table 2. Circular dichroism results of the wild-type Cry3Aa and disulfide mutant proteins.

	Wild-type	DS1	DS2	DS3
$[\theta]_{220}/[\theta]_{208}$	1.18	0.92	1.34	1.34
T_m (˚C)	57.3	67.3	71.4	70.8

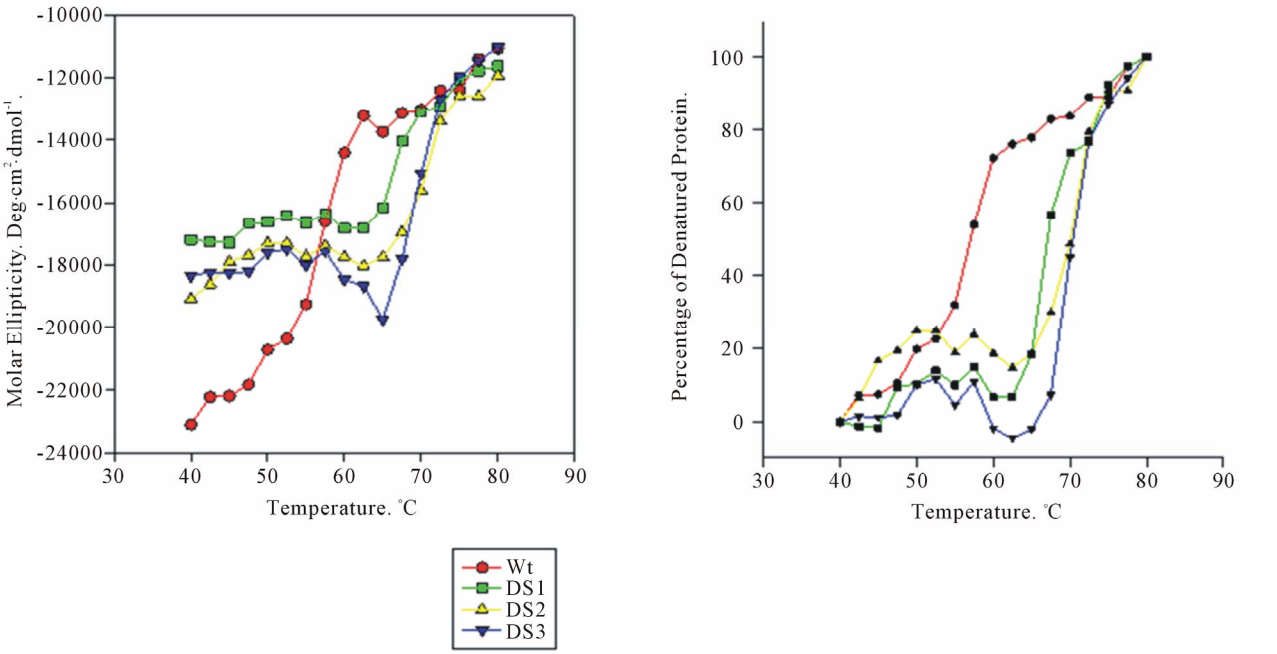

Figure 4. Thermal stability of wild-type Cry3Aa and the double-cysteine mutant proteins. (a) CD thermal equilibrium transition profiles, recorded at 222 nm, were normalized to the fraction of folded protein. Melting was performed in 10 mM sodium carbonate buffer (pH 11.0) at a rate 6˚C/h. Melting temperatures are illustrated by dashed lines; (b) Thermal denaturation curves for Cry3Aa wild type (●), and the three double cysteine mutants DS1 (■), DS2 (▲) and DS3 (▼).

around 250 nm as a function of temperature if disulfide bonds were formed (**Figure 5**). Note that the thermal stability of the disulfide mutants varies approximately linearly with the increase of temperature. It is noteworthy that DS1 and DS3 mutant proteins display an increase in absorptivity at 250 nm, compared to wild-type and DS2 proteins. These results would suggest a large contribution of these two double-cysteine mutations to the thermal stability of the Cry3Aa protein, which is consistent with formation of disulfide bridges.

3.5. Insecticidal Activity of Mutant Proteins

To determine whether these mutations affect the toxicity of the Cry3Aa δ-endotoxin, the toxicities of the wild-type and mutant toxins towards *T. molitor* larvae were analyzed by a force-feeding method. The results are reported in **Table 1**. The LD_{50} (50% lethal dose) for wild-type protein was 11.4 µg/larva. Single mutant, $V_{276}C$, showed slightly less toxicity than the wild-type, but the confidence intervals overlapped. The toxicity of the DS3 mutant, $A_{198}C/V_{276}C$, was similar to that of the wild-type toxin (LD_{50} = 9.6 µg/larva, 95% confidence limits: 6.0 - 18.6 µg). Overall, The LD_{50} values showed no significant difference in insecticidal activity between the wild-type and mutant proteins (**Table 1**).

4. DISCUSSION

Three double cysteine mutants were engineered into the beetle-active δ-endotoxin Cry3Aa. Two of the double mutants (DS2 and DS3) were expected to create disulfide bonds connecting the central α-helix 5 to an outer helix (α-helix 7), and the other double mutant (DS1) was expected to link another outer chain (α-helix 2) to the α-helix 5. The data indicate that these double mutations resulted in increased structural stability of the proteins. In contrast, the single cysteine mutant, $F_{193}C$, did not produce structurally-stable protein (**Figure 2**, **lane 3**). Another single mutant, $V_{276}C$, was slightly more susceptible to proteolysis than both the wild-type and the other mutant proteins (**Figure 2**, **lane 5**), although why these individual cysteine mutations had an unfavorable effect on stability is not known. It is noted, however, that both F_{193} and V_{276} are buried in the hydrophobic interior of domain I [11]. Thus, the effects of the $F_{193}C$ and $V_{276}C$ mutations might be attributed to the removal of favorable hydrophobic interactions involving the native phenylalanine and valine residues at these positions. Interestingly, the unfavorable effects of the single-cysteine mutants are suppressed in the double-cysteine mutations, a clear indication of the formation of disulfide bonds, and DS1, DS2, and DS3 produced structurally stable proteins (**Figure 2**, **lanes 7-9**).

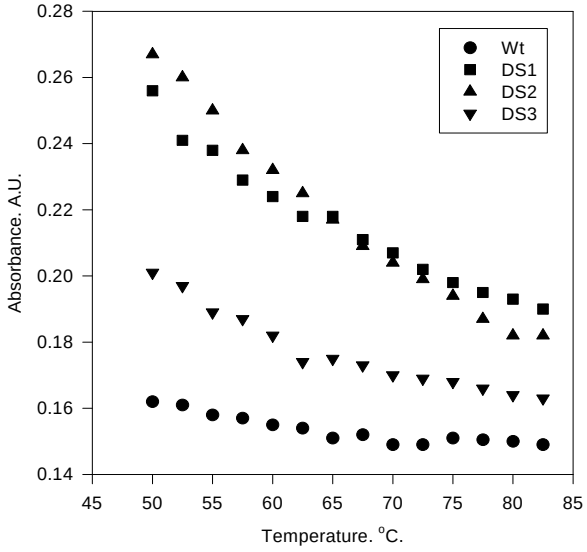

Figure 5. Guanidine hydrochloride induced unfolding of wild-type Cry3Aa and double cysteine mutant proteins. Far-UV spectra were recorded at 250 nm for proteins in 6 M GnHCl. Thermal denaturation curves were performed in 10 mM sodium carbonate buffer (pH 11.0).

Toxicity assays of the mutant proteins on *T. molitor* larvae showed that neither the proteins with single-cysteine substitutions, nor the double-cysteine mutants had a significant effect on the insecticidal activity, as compared to wild-type toxin (**Table 1**). The single-cysteine mutant proteins, when ingested by beetle larvae, were as toxic as the wild-type toxin, with overlapping confidence limits (**Table 1**). Since the midgut environment of beetle larva is usually mildly acidic and exhibits a negative (reducing) redox potential [34], disulfide bonds of mutant proteins may be labile under these conditions. This would explain why the LD_{50} values for double mutants were similar to wild-type protein. However, we cannot rule out the possibility that buried disulfide bridges may not be exposed to the reducing environment of the midgut lumen. In this case, a plausible explanation is that the entire domain I inserts into membrane as previously proposed, either as a whole protein [7,12-17] or as a member of an oligomeric complex [18, 23,35,36]. This would also result in no difference in toxicity between the wild-type and disulfide proteins. Thus, it is a reasonable assumption that the whole bundle of α-helices may be maintained as a closely-packed domain by disulfide bonds.

Analysis of the difference between the ellipticity for wild-type and DS mutant proteins indicates that the decrease in the parallel band maximum for the DS2 and DS3 mutants (**Figure 3**) corresponds to the conversion of a relatively loose α-helical bundle to a more close-packed structure. It therefore appears reasonable to conclude that disulfide bridges were formed between the α-helices 5 and 7 resulting in a more tightly packed con-

formation of domain I. Nevertheless, we did not observe a similar result for DS1, where the double cysteine mutations would have been expected to hold α-helices 2 and 5 together (**Table 2**).

To further characterize the properties of the double-cysteine mutations, a geometry optimization for the DS1, DS2, and DS3 mutant proteins was performed using the AMBER algorithm [24]. The details of the potential disulfide bond geometry in the mutant proteins are summarized in **Table 3**. There are stringent geometric requirements for the relative positions and orientations of the two cysteine residues in order to form stable disulfide bridges [6]. The bond length must be 2.05 ± 0.03 Å, and the optimal χ_3 dihedral torsion angle should be ± 90 degrees. Based on the simulation, the disulfide bond in the DS3 mutant ($A_{198}C/V_{276}C$) almost invariably satisfies these criteria. These calculated data for DS3 mutant are in good agreement with thermal denaturation CD spectra and the 250 nm UV absorbance results.

The thermal CD transition curves for the mutant proteins suggest that there is a covalent linkage between the central α-helix 5 and the outer chains which significantly increases protein stability. The DS mutant proteins displayed higher stability against temperature and chemical (GnHCl) denaturation than the wild-type protein. Thermal CD transition curves exhibit a 10˚C to 14˚C difference in melting temperature (**Figure 4** and **Table 2**), which reflects a stabilizing effect that can be explained by the engineered inter-chain bridges. In addition UV spectra taken in the presence of GnHCl also indicate a substantial increase in protein stability that could result from disulfide bonds (**Figure 5**). The difference in the 250-nm UV absorbance between DS2 and DS3, however, was unexpected. The decrease in intensity for DS2 is not consistent with the $[\theta]_{220}/[\theta]_{208}$ ratio and the melting temperature (**Table 2**).

5. CONCLUSION

The thermal analysis data, the molecular calculations, and the structural analysis indicate that the double-cysteine mutant proteins DS1 and DS3 formed disulfide bridges. In addition, the fact that DS1 became a stable protein only after a second mutation was introduced further supports this conclusion. It is also clear that there is not conclusive evidence to indicate that the DS2 mutant formed a disulfide bridge. Taken together these results indicate that we have introduced two stable disulfide bonds into Cry3Aa, but that these mutations do not alter protein toxicity. A plausible model to explain these observation will be one in which the protein inserts into the target membrane either as a whole molecule, or as a

Table 3. Details of disulfide bond geometry in the mutant toxins by geometry optimization.

Proteins	Distance (Å)			Disulfide bond torsion angle* (˚)					Energy
	C_a-C'$_a$	C_b-C'$_b$	S-S'	c_1	c_2	c_3	c'$_2$	c'$_1$	
									(kcal/mol)
DS1 mutant									
$M_{110}C/F_{193}C$	4.87	4.60	2.01	−139	84	−144	77	−121	−342
(Wild-type)#	(6.12)	(7.21)							
DS2 mutant									
$T_{195}C/V_{276}C$	5.68	4.34	2.03	−118	64	152	53	−96	−263
(Wild-type)	(6.03)	(5.92)							
DS3 mutant									
$A_{198}C/V_{276}C$	5.81	3.60	2.04	−175	154	93	65	177	−362
(Wild-type)	(5.81)	(4.29)							

*The geometry of a disulfide bond is represented by five torsion angles, as shown below:

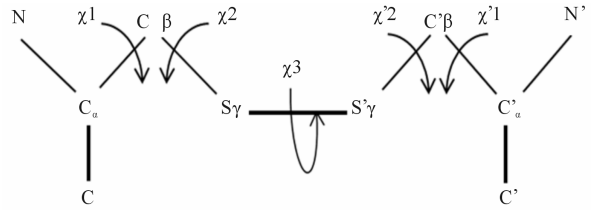

#Corresponding distances in the wild-type Cry3A crystal structure are given in parentheses.

member of a complex oligomeric structure.

6. ACKNOWLEDGEMENTS

We would like to thank Dr. Carol E. Parker of the UVic-Genome BC Proteomics Centre for critical review of this manuscript.

REFERENCES

[1] Privalov, P.L. and Gill, S.J. (1988) Stability of protein structure and hydrophobic interaction. *Advances in Protein Chemistry*, **39**, 191-234. doi:10.1016/S0065-3233(08)60377-0

[2] Horovitz, A., Serrano, L., Avron, B., Bycroft, M. and Fersht, A.R. (1990) Strength and co-operativity of contributions of surface salt bridges to protein stability. *Journal of Molecular Biology*, **21**, 1031-1044. doi:10.1016/S0022-2836(99)80018-7

[3] Burley, S.K. and Petsko, G.A. (1988) Weakly polar interactions in proteins. *Advances in Protein Chemistry*, **39**, 125-189. doi:10.1016/S0065-3233(08)60376-9

[4] Stickle, D.F., Presta, L.G., Dill, K.A. and Rose, G.D. (1992) Hydrogen bonding in globular proteins. *Journal of Molecular Biology*, **226**, 1143-1159. doi:10.1016/0022-2836(92)91058-W

[5] Creighton, T.E. (1988) Disulphide bonds and protein stability. *Bioessays*, **8**, 57-63. doi:10.1002/bies.950080204

[6] Anfinsen, C.B. (1973) Principles that govern the folding of protein chains. *Science*, **181**, 223-230. doi:10.1126/science.181.4096.223

[7] Alzate, O., You, T., Claybon, M., Osorio, C., Curtiss, A. and Dean, D.H. (2006) Effects of disulfide bridges in domain I of *Bacillus thuringiensis* Cry1Aa *δ*-endotoxin on ion-channel formation in biological membranes. *Biochemistry*, **45**, 13597-13605. doi:10.1021/bi061474z

[8] Schwartz, J.L., Juteau, M., Grochulski, P., *et al*. (1997) Restriction of intramolecular movements within the Cry1Aa toxin molecule of *Bacillus thuringiensis* through disulfide bond engineering. *FEBS Letters*, **410**, 397-402. doi:10.1016/S0014-5793(97)00626-1

[9] Thornton, J.M. (1981) Disulphide bridges in globular proteins. *Journal Molecular Biology*, **151**, 261-287. doi:10.1016/0022-2836(81)90515-5

[10] Hodgman, T.C. and Ellar, D.J. (1990) Models for the structure and function of the *Bacillus thuringiensis* delta-endotoxins determined by compilational analysis. *DNA Sequence*, **1**, 97-106.

[11] Li, J.D., Carroll, J. and Ellar, D.J. (1991) Crystal structure of insecticidal delta-endotoxin from *Bacillus thuringiensis* at 2.5 Å resolution. *Nature*, **353**, 815-821. doi:10.1038/353815a0

[12] Alzate, O., Hemann, C.F., Osorio, C., Hille, R. and Dean, D.H. (2009) Ser170 of *Bacillus thuringiensis* Cry1Ab delta-endotoxin becomes anchored in a hydrophobic moiety upon insertion of this protein into *Manduca sexta* brush border membranes. *BMC Biochemistry*, **10**, 25-34. doi:10.1186/1471-2091-10-25

[13] Aronson, A. (2000) Incorporation of protease K into larval insect membrane vesicles does not result in disruption of integrity or function of the pore-forming *Bacillus thuringiensis δ*-endotoxin. *Applied Environmental Microbiology*, **66**, 4568-4570. doi:10.1128/AEM.66.10.4568-4570.2000

[14] Arnold, S., Curtiss, A., Dean, D. H. and Alzate, O. (2001) The role of a proline-induced broken-helix motif in R-helix 2 of *Bacillus thuringiensis δ*-endotoxins. *FEBS Letters*, **490**, 70-74. doi:10.1016/S0014-5793(01)02139-1

[15] Loseva, O.I., Tiktopulo, E.I., Vasiliev, V.D., Nikulin, A.D., Dobritsa, A.P. and Potekhin, S.A. (2001) Structure of Cry3A *δ*-endotoxin within phospholipid membranes. *Biochemistry*, **40**, 14143-14151. doi:10.1021/bi010171w

[16] Nair, M.S. and Dean, D.H. (2008) All domains of Cry1A toxins insert into insect brush border membranes. *Journal Biological Chemistry*, **283**, 26324-26331. doi:10.1074/jbc.M802895200

[17] Potekhin, S.A., Loseva, O.I., Tiktopulo, E.I. and Dobritsa, A.P. (1999) Transition state of the rate-limiting step of heat denaturation of Cry3A *δ*-endotoxin. *Biochemistry*, **38**, 4121-4127. doi:10.1021/bi982789k

[18] Jimenez-Juarez, N., Munoz-Garay, C., Gomez, I., *et al*. (2007) *Bacillus thuringiensis* Cry1Ab mutants affecting oligomer formation are non-toxic to *Manduca sexta larvae*. *Journal of Biological Chemistry*, **282**, 21222-21229. doi:10.1074/jbc.M701314200

[19] Girard, F., Vachon, V., Prefontaine, G., *et al*. (2008) Cysteine scanning mutagenesis of a4, a putative porelining helix of the *Bacillus thuringiensis* insecticidal toxin Cry1Aa. *Applied Environmental Microbiology*, **74**, 2565-2572. doi:10.1128/AEM.00094-08

[20] Vachon, V., Prefontaine, G., Rang, C., *et al*. (2004) Helix 4 mutants of the *Bacillus thuringiensis* insecticidal toxin Cry1Aa display altered pore-forming abilities. *Applied Environmental Microbiology*, **70**, 6123-6130. doi:10.1128/AEM.70.10.6123-6130.2004

[21] Florez, A.M., Osorio, C. and Alzate, O. (2012) Protein engineering of *Bacillus thuringiensis δ*-endotoxins. In: Sansinenea, E., Ed., *Bacillus thuringiensis Biotechnology*, Springer-Verlag, New York, 350.

[22] Laflamme, E., Badia, A., Lafleur, M., Schwartz, J.L. and Laprade, R. (2008) Atomic force microscopy imaging of *Bacillus thuringiensis* Cry1 toxins interacting with insect midgut apical membranes. *Journal of Membranes Biology*, **222**, 127-139.

[23] Groulx, N., McGuire, H., Laprade, R., Schwartz, J.-L. and Blunk, R. (2011) Single molecule fluorescence study of the *Bacillus thuringiensis* toxin Cry1Aa reveals tetramerization. *Journal of Biological Chemistry*, **286**, 42274-42282. doi:10.1074/jbc.M111.296103

[24] Weiner, S.J. and Kollman, P.A. (1986) An all atom force field for simulations of proteins and nucleic acids. *Journal of Computational Chemistry*, **7**, 230-252. doi:10.1002/jcc.540070216

[25] Wu, S.J. and Dean, D.H. (1996) Functional significance of loops in the receptor binding domain of *Bacillus thuringiensis* CryIIIA delta-endotoxin. *Journal of Molecular Biology*, **255**, 628-640. doi:10.1006/jmbi.1996.0052

[26] Kunkel, T.A. (1985) Rapid and efficient site-specific mutagenesis without phenotypic selection. *Proceedings of National Academic Science USA*, **82**, 488-492. doi:10.1073/pnas.82.2.488

[27] Laemmli, U.K. (1970) Cleavage of structural proteins during the assembly of the head of bacteriophage T4. *Nature*, **227**, 680-685. doi:10.1038/227680a0

[28] Berova, N., Nakanishi, K. and Woody, R. (2000) Circular dichroism: Principles and applications. 2nd Edition, Wiley-VCH, New York

[29] Greenfield, N.J. (2006) Using circular dichroism spectra to estimate protein secondary structure. *Nature Protocols*, **1**, 2876-2890. doi:10.1038/nprot.2006.202

[30] Cooper, T.M. and Woody, R.W. (1990) The effect of conformation on the CD of interacting helices: A theoretical study of tropomyosin. *Biopolymers*, **30**, 657-676. doi:10.1002/bip.360300703

[31] Zhou, N.E., Kay, C.M. and Hodges, R.S. (1992) Synthetic model proteins. Positional effects of interchain hydrophobic interactions on stability of two-stranded alpha-helical coiled-coils. *Journal of Biological Chemistry*, **267**, 2664-2670.

[32] Wetlaufer, D.B. (1962) Ultraviolet spectra of proteins and amino acids. *Advances in Protein Chemistry*, **17**, 303-390. doi:10.1016/S0065-3233(08)60056-X

[33] Monera, O.D., Kay, C.M. and Hodges, R.S. (1994) Protein denaturation with guanidine hydrochloride or urea provides a different estimate of stability depending on the contributions of electrostatic interactions. *Protein Science*, **3**, 1984-1991. doi:10.1002/pro.5560031110

[34] Murdock, L.L., Brookhart, G.L., Dunn, P.E., *et al*. (1987) Cysteine digestive proteinases in Coleoptera. *Computational Biochemistry Physiology*, **87**, 783-787. doi:10.1016/0305-0491(87)90388-9

[35] Bravo, A., Gomez, I., Conde, J. *et al*. (2004) Oligomerization triggers binding of a *Bacillus thuringiensis* Cry1Ab pore-forming toxin to aminopeptidase N receptor leadingto insertion into membrane microdomains. *Biochemistry*, *Biophysics Acta*, **1667**, 38-46. doi:10.1016/j.bbamem.2004.08.013

[36] Jimenez-Juarez, N., Munoz-Garay, C., Gomez, I., Gill, S.S., Soberon, M. and Bravo, A. (2008) The pre-pore from *Bacillus thuringiensis* Cry1Ab toxin is necessary to induce insect death in *Manduca sexta*. *Peptides*, **29**, 318-323. doi:10.1016/j.peptides.2007.09.026

